Swash saturation

is it universal and do we have an appropriate model?

Hughes, Michael; Baldock, Tom; Aagaard, Troels

Published in:
Proceedings Coastal Dynamics 2017

Publication date:
2017

Document version
Publisher's PDF, also known as Version of record

Citation for published version (APA):
Hughes, M., Baldock, T., & Aagaard, T. (2017). Swash saturation: is it universal and do we have an appropriate model? In T. Aagaard, R. Deigaard, & D. Fuhrman (Eds.), *Proceedings Coastal Dynamics 2017* (pp. 192-203)

Swash saturation: is it universal and do we have an appropriate model?

Hughes, Michael; Baldock, Tom; Aagaard, Troels

Published in:
Proceedings Coastal Dynamics 2017

Publication date:
2017

Citation for published version (APA):
Hughes, M., Baldock, T., & Aagaard, T. (2017). Swash saturation: is it universal and do we have an appropriate model? In T. Aagaard, R. Deigaard, & D. Fuhrman (Eds.), Proceedings Coastal Dynamics 2017 (Chapter 108, pp. 192-203)

Coastal Dynamics 2017
Paper No.108

SWASH SATURATION: IS IT UNIVERSAL AND DO WE HAVE AN APPROPRIATE MODEL?

Michael G. Hughes[1], Tom E. Baldock[2] and Troels Aagaard[3]

Abstract

An extensive field data set representing the full range of micro-tidal beach states (reflective, intermediate and dissipative) is used to investigate swash saturation. Two models that predict the behavior of saturated swash are tested: one driven by standing waves and the other driven by bores. Despite being based on entirely different premises, they predict similar trends in the limiting (saturated) swash height with respect to dependency on frequency and beach gradient. For a given frequency and beach gradient, however, the bore-driven model predicts a larger saturated swash height by a factor 2.5. Both models broadly predict the general behaviour of swash saturation evident in the data, but neither model is accurate in detail. While swash saturation in the short wave frequency band is common on some beach types, it does not always occur across all beach types.

Key words: swash zone, surf zone, energy saturation, beach type, beach morphodynamics

1. Introduction

Swash (shoreline oscillations) on natural beaches occurs across a broad range of frequencies, driven by a variety of incident wave forms. Swash spectra are typically discussed with respect to two frequency bands that correspond to short waves and long (infragravity) waves incident at the beach face. Short wave swash derives from locally-generated wind waves and from swell (e.g., Waddell, 1976; Hughes, 1992; Holland and Puleo, 2001), whereas infragravity swash includes leaky-mode standing waves and edge waves (e.g., Huntley, 1976; Aagaard, 1991; Holland et al., 1995; Holland and Holman, 1999). A fundamental difference between incident short waves and most surf zone long waves is that the former usually break before reaching the beach face, whereas the latter usually do not, except possibly on very mild slopes under energetic conditions (Battjes et al., 2004).

Guza and Thornton (1982), and subsequent authors (e.g., Holman, 1983; Aagaard, 1990), have presented field measurements on dissipative type beaches clearly showing the infragravity swash height increasing with offshore wave height while the short wave swash height remained roughly constant and thus saturated. We specifically define saturation here to mean that the swash height calculated from the shoreline elevation time series variance, or equivalently the spectral energy, remains constant in a specified frequency band under increasing offshore (incident) wave energy. This requires that 'excess' energy, defined as the proportion of incident wave energy over and above that corresponding to the saturated swash energy, must be dissipated or reflected prior to influencing the magnitude of the shoreline motion.

Huntley et al. (1977) proposed on the basis of Miche's (1944; 1951) model for wave behaviour in the surf zone that swash might be universally saturated in the short wave band and, if so, that the swash spectrum will display an energy roll-off rate of f^{-4}. Using a different model premise based on Shen and Meyer (1963), Mase (1998) and Baldock and Holmes (1999) also proposed that saturated swash spectra should have the same energy roll-off rate. Further details of these models are presented in Section 2.

Over the past three decades studies have demonstrated or indicated swash saturation occurred in the short wave frequency band (f<0.05 Hz) on particular beaches and some have also indicated swash saturation extended into the infragravity band on particular beaches (e.g., Guza and Thornton, 1982;

[1] Water Wetlands and Coasts Science, NSW Office of Environment & Heritage, Australia. michael.hughes@environment.nsw.gov.au
[2] School of Civil Engineering, University of Queensland, Australia. t.baldock@uq.edu.au
[3] Institute of Geosciences and Natural Resources, University of Copenhagen, Denmark. taa@ign.ku.dk

Raubenheimer and Guza, 1996; Ruessink et al., 1998; Holland and Holman, 1999; Ruggiero et al., 2004; Senechal et al., 2011; Guedes et al., 2013; Hughes et al., 2014). To our knowledge, however, there has been no systematic investigation of the process across all beach types. This contribution uses the extensive data set previously described in Hughes et al. (2014) to investigate swash saturation across a wide range of wave and beach conditions including the reflective, intermediate and dissipative beach types described by Wright and Short (1984).

2. Background

2.1. *Standing wave swash model*

The ratio of wave steepness to beach profile slope is fundamental to wave breaking. The limiting condition for non-breaking waves can be determined from the non-linear shallow water theory applied to standing long waves (Carrier and Greenspan, 1958)

$$\varepsilon = \frac{a_s \omega^2}{g\beta^2} \tag{1}$$

where a_s is vertical swash amplitude, ω is wave radian frequency ($2\pi f$ where f is frequency), g is gravitational acceleration and β is beach slope angle in radians (assumed here to be small enough for $\tan\beta \approx \sin\beta \approx \beta$). When the value of the swash scaling parameter ε equals or exceeds the critical value ε_c=1 then wave breaking occurs.

Miche's (1944; 1951) model for monochromatic swash states that the amplitude of shoreline oscillations is proportional to the standing wave amplitude. With increasing incident wave amplitude, the shoreline amplitude will also increase up to the value corresponding with the maximum possible standing wave amplitude for the given frequency and beach slope. Beyond this value the increased incident energy is hypothesized to be dissipated entirely by wave breaking. This implies the swash becomes saturated with the onset of wave breaking. According to Miche's (1944; 1951) model, swash should therefore be saturated for values of $\varepsilon_c \geq 1$. Substituting $Z=2a_s$ and ε_c=1 into equation (1) yields the limiting (saturated) swash height Z under monochromatic standing wave conditions:

$$Z = \frac{g\beta^2}{2(\pi f)^2} \tag{2}$$

Huntley et al. (1977) further developed the monochromatic model to suit broad-banded conditions and proposed that the shoreline run-up spectrum across the frequency band corresponding to breaking waves might be universally described by

$$E(f) = \left[\frac{\hat{\varepsilon}_c g\beta^2}{(2\pi f)^2}\right]^2 \tag{3}$$

where E is energy density, and $\hat{\varepsilon}_c$ is the critical value of the swash scaling parameter marking the onset of wave breaking and swash saturation. Here $\hat{\varepsilon}_c$ is in dimensional form with units of $\mathrm{Hz}^{-½}$. We make a clear distinction herein between what we will term the monochromatic and the broad-banded standing wave model for swash. The former relates to Miche's model and the limiting swash height for a specific frequency is given by equation (2) ($\varepsilon=\varepsilon_c$=1), whereas the latter is related to Huntley et al's modification of Miche's model to suit broad-banded conditions and the limiting swash energy density across the frequency bandwidth that wave breaking occurs is given by equation (3). That is, across the frequency bandwidth for which combinations of a_s and ω yield $\hat{\varepsilon}_c$ values consistent with wave breaking, i.e., $\varepsilon \geq \varepsilon_c$. Based on five spectra from natural beaches representing a factor 2 range of beach gradients from 0.065 to 0.13, Huntley

et al. (1977) suggested that $\hat{\varepsilon}_c$ has a value somewhere between 2 and 3 Hz$^{-½}$.

It is not a trivial matter to relate $\hat{\varepsilon}_c$ to its monochromatic equivalent ε_c. Based on the fact that the down-slope acceleration of the shoreline cannot exceed the down-slope acceleration due to gravity, Huntley et al. (1977) developed an argument which concluded that $\varepsilon_c \equiv \hat{\varepsilon}_c\sqrt{\Delta f}$, where Δf (Hz) is the bandwidth over which wave breaking is occurring. The values of Δf and β are expected to co-vary inversely such that $\hat{\varepsilon}_c$ universally remains a constant value of unity.

2.2. *Bore-driven swash model*

Using a monochromatic and friction-less ballistic model for the shoreline motion driven by bores (Shen and Meyer, 1963), Baldock and Holmes (1999) derived a different formulation for the limiting (saturated) swash height. They defined the onset of saturation to occur when the swash cycle from one bore does not complete before the arrival of the following bore, thus the shoreline excursion of one or both is reduced.

This is equivalent to the 'phase difference' concept introduced by Kemp (1975). For a given monochromatic incident bore frequency there exist combinations of swash height (or bore height) and beach slope that result in the shoreline frequency being higher than the bore frequency (unsaturated swash), and there exist combinations that would result in the shoreline frequency being lower than the incident bore frequency, and consequently bore-swash interaction occurs (saturated swash).

The initial speed of the shoreline at bore collapse, U_o, is assumed to be related to the collapsing bore and typically takes the form

$$U_o = C\sqrt{gH_b} \tag{4}$$

where H_b is the bore height at the shoreline and C is a coefficient that describes the efficiency of bore collapse; equal to 2 for complete conversion of potential to kinetic energy (Yeh et al., 1989). From the ballistic model for shoreline motion, the frequency of a swash cycle is (Baldock and Holmes, 1999)

$$f = \frac{g\beta}{2C\sqrt{gH_b}} \tag{5}$$

Applying the ballistic model prediction that the swash height is $U_0^2/2g = C^2H_b/2$ and the argument that the swash is saturated when the swash frequency becomes less than or equal to the bore frequency, the limiting swash height is (Baldock and Holmes, 1999)

$$Z = \frac{g\beta^2}{8f^2} \tag{6}$$

Equation (6) is analogous to equation (2) in that the former defines the limiting swash height for a specific frequency driven by standing waves and the latter defines the same for swash driven by bores. Comparing equations (2) and (6), the limiting swash height produced by bores is approximately 2.5 times that produced by the largest non-breaking standing wave of equivalent frequency.

There is no obvious pathway for extending the monochromatic theory for bore-driven swash to suit broad-banded conditions. A broad-banded version of equation (6) would predict the saturated swash energy level to be proportional to the beach gradient to the power 4 and the frequency to the power -4 (see Baldock and Holmes, 1999), consistent with the standing wave model (cf. equation 3), but it is unclear what the dimensionally correct coefficient would be.

2.3. *Summary of model predictions*

There is an important distinction between the two models for saturated swash. The standing wave model describes depth-limited saturation of short waves in the inner surf zone, thereby limiting swash energy in

the short wave band. In this case 'excess' short wave energy is dissipated by turbulent breaking across the surf zone. The bore model describes swash saturation through dissipation of 'excess' energy by turbulence and/or opposing flows associated with wave-swash interactions. There is no requirement in this case for waves in the surf zone to be depth-limited or saturated.

The monochromatic version of both models predict a direct dependency of the saturated swash height on beach gradient squared and inverse dependency on frequency squared. Equivalently, the spectral versions of the models predict a direct dependency of the saturated energy density on beach gradient to the fourth power and inverse dependency on frequency to the fourth power. The latter results in the characteristic f^{-4} roll-off region in swash spectra.

Many studies have presented swash spectra displaying an f^{-4} roll-off region in the short wave frequency band and some extending into the infragravity wave band (e.g., Guza and Thornton, 1982; Raubenheimer and Guza, 1996; Ruessink et al., 1998; Holland and Holman, 1999; Ruggiero et al., 2004; Senechal et al., 2011; Guedes et al., 2013; Hughes et al., 2014). Guza and Thornton (1982) presented additional analysis that was independent of the spectral roll-off to demonstrate swash saturation. They measured the significant swash height in the short wave frequency band over a factor 3 range in offshore significant wave height and showed that the former was constant in their experiment. Similarly, Raubenheimer and Guza (1996) showed that the significant swash height in the short-wave frequency band increased with the beach gradient squared in their experiment.

3. Field Sites, Methods and Data

A full description of the field sites and methods used for measuring the shoreline elevation time series and calculating the swash spectra reported here are provided in Hughes et al. (2014). Only the salient points and new information are provided below.

The field sites were located in Australia and Denmark. All beaches studied were micro-tidal and composed predominantly of sand ranging from very fine to very coarse. Beach gradients, calculated as the average gradient over the active swash zone, ranged across nearly an order of magnitude from 0.017 to 0.164. Offshore significant wave heights ranged from 0.5 m to 3.0 m. All three major beach types (reflective, intermediate and dissipative) are represented in the data set.

Shoreline elevation time series were measured using either a resistance-type runup wire or video imagery. Data were compiled into 15 minute time series (runs) to ensure stationarity with respect to the tide, and were digitized (re-sampled where necessary) to have a consistent sampling frequency of 10 Hz across the data set. All calculated spectra had 22 degrees of freedom and a frequency resolution of 1.11×10^{-3} Hz.

The lowest frequency to which the f^{-4} roll-off region extended, f_s, was determined for each spectrum in the following way. The best fit linear regression line (and 95% confidence interval) was fitted to that part of the spectrum displaying an f^{-4} roll-off. The regression line was then extended in the down-frequency direction, and the value of f_s was taken as the frequency at which the spectrum departed significantly from the regression line; that is, outside the confidence interval (see also Ruessink et al., 1998). The width of the f^{-4} roll-off band, Δf, was then calculated using $\Delta f = 0.5 - f_s$.

The analysis presented here extends that previously presented in Hughes et al. (2014) to include analysis of the shoreline elevation time series on a wave-by-wave basis. This required identification of all shoreline maxima and minima in each time series. Shoreline maxima were automatically identified by zero-down crossings of the first derivative of the time series. Shoreline minima were then identified as the minimum elevation between successive shoreline maxima.

The individual swash height Z for each swash cycle was calculated as the elevation difference between each shoreline minimum and its following maximum. The frequency associated with that swash cycle was calculated as the inverse of two times the difference between the shoreline minimum and its following maximum. Swash cycles were only considered significant and included in the analysis if their frequencies were less than 0.25 Hz.

The combined Australian and Danish data set includes 36 separate field deployments across nine beaches; yielding 187 runs (15-minute time series), 187 swash spectra and 13,150 individual swash cycles. This has been supplemented with examples from other studies to demonstrate consistency (Raubenheimer and Guza, 1996; Ruessink et al., 1998; Ruggiero et al., 2004; Senechal et al., 2011; Guedes et al., 2013).

Previously published swash spectra have been used to estimate a value for $\hat{\varepsilon}_c$ and Δf. This was done by reading off the energy density E for a specific frequency f in the f^{-4} roll-off region of the published swash spectra. The estimated E and f together with the published beach gradient β were substituted into equation (3) to determine $\hat{\varepsilon}_c$. The lowest frequency to which the f^{-4} roll-off region extended, f_s, was estimated by eye, and then Δf was calculated using Δf=0.5-f_s. There are two estimates for $\hat{\varepsilon}_c$ and Δf from Ruggiero et al. (2004), one from their Region I and Region II. There are also two estimates from Raubenheimer and Guza (1996), because they provided a wide range of foreshore slopes, 0.04 and 0.11.

4. Results

Numerous previous studies have measured swash spectra displaying an f^{-4} roll-off region at the high frequency end of the spectrum (Section 2). In a previous analysis of the data presented here the roll-off region was observed ubiquitously across all beach types and a wide range of wave conditions (Hughes et al., 2014). That analysis also explored aspects of the broad-banded standing wave model for swash and those results are briefly repeated here for convenience, together with the inclusion of additional analysis.

Equation (3) can be re-written in the simpler form

$$E(f) = \alpha f^{-4} \tag{7}$$

where the proportionality coefficient α is

$$\alpha = \frac{\hat{\varepsilon}_c^2 g^2 \beta^4}{(2\pi)^4} \tag{8}$$

Re-arranging equation (8) to

$$\sqrt{\alpha} = \hat{\varepsilon}_c \sqrt{\frac{g^2 \beta^4}{2\pi^4}} \tag{9}$$

shows that the slope of the regression line between measured values of $\sqrt{\alpha}$ and $\sqrt{[g^2\beta^4(2\pi)^{-4}]}$ will yield a value for $\hat{\varepsilon}_c$. A value for α was obtained for each available spectrum as the slope of the linear regression line between E and f^{-4} over a common frequency range that was inside the roll-off band for all spectra (i.e. 0.15-0.25 Hz). Most of the regression lines had an r^2-value greater than 0.8, only three were less than 0.5, and only one was not significant at the 95% confidence interval (see Hughes et al. 2014 for more details).

The value of $\sqrt{\alpha}$ for each of the 187 spectra are plotted against $\sqrt{[g^2\beta^4(2\pi)^{-4}]}$ in Figure 1. Considerable scatter exists in the data, but it appears that the swash energy level in the f^{-4} roll-off band scales with β^4. Given the high power some scatter may relate to the precision with which the beach gradient can be estimated. The fitted linear regression line has an associated r^2=0.68 (p=0.000), which is significant at the 95% confidence level, and the slope of the regression lines yields $\hat{\varepsilon}_c$=2.75±0.22 Hz $^{-½}$. Ignoring the data from dissipative beaches has a minimal impact on the estimated value of $\hat{\varepsilon}_c$ (viz. $\hat{\varepsilon}_c$=2.76±0.26 Hz $^{-½}$).

The data shown from other published studies demonstrates a similar trend. The data reported by Raubenheimer and Guza (1996) and Senechal et al. (2011), from relatively steeper beaches, are well within the scatter of the Hughes et al. (2014) data set. Whereas the data from Ruggiero et al. (2004) and Guedes et al. (2013) extend the data coverage down to lower gradient beaches.

Individual estimates of the non-dimensional form of $\hat{\varepsilon}_c$ for each available spectrum, $\hat{\varepsilon}_c\sqrt{\Delta f}$, are plotted against beach gradient in Figure 2. Consistent with theoretical expectation, the values of $\hat{\varepsilon}_c\sqrt{\Delta f}$ are approximately constant for most of the data set. Excluding the low-gradient, dissipative beaches where $\hat{\varepsilon}_c\sqrt{\Delta f}$ exceeded 5 and reached >30, the mean value of $\hat{\varepsilon}_c\sqrt{\Delta f}$ (with 95% confidence interval) was 2.25±1.72. Again, the data from other published studies is consistent with the trend of the Hughes et al. (2014) data. The theoretical expectation that the values of Δf and β co-vary such that $\hat{\varepsilon}_c$ remains a constant is also broadly evident in the data (Figure 3).

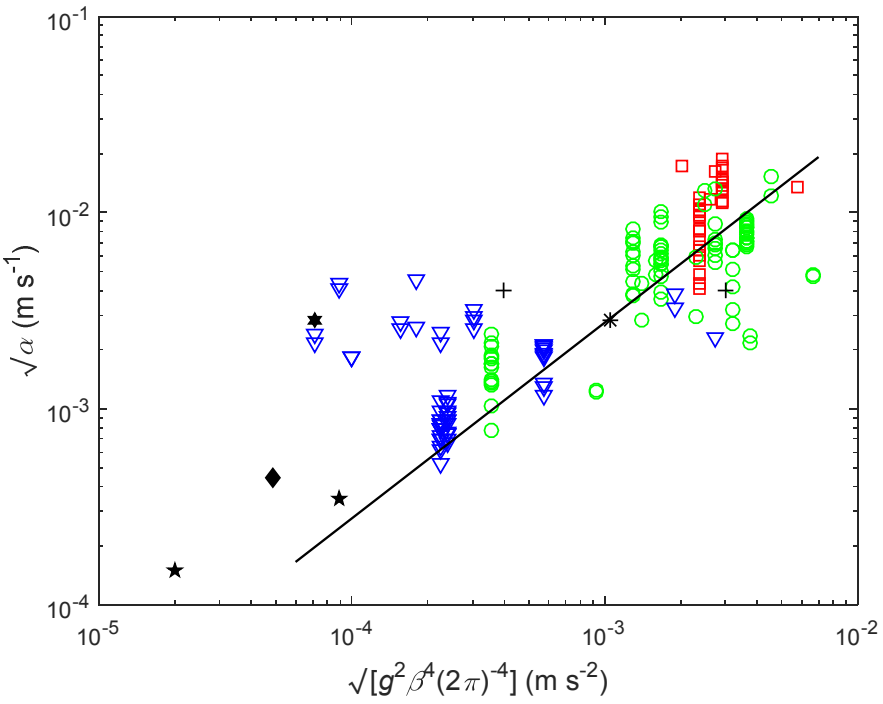

Figure 1: Scatter plot of data used to estimate $\hat{\varepsilon}_c$. Values on the axes are explained in the text. Coloured symbols identify beach-states: reflective (red squares), intermediate (green circles) and dissipative (blue triangles). Black symbols identify data from other studies: Raubenheimer and Guza (1996) (black crosses), Ruessink et al. (1998) (black hexagon), Ruggiero et al. (2004) (black pentagons), Senechal et al. (2011) (black asterisk) and Guedes et al. (2013) (black diamond). The solid line represents the linear least-squares regression model fitted only to the data from this study (After Hughes et al., 2014).

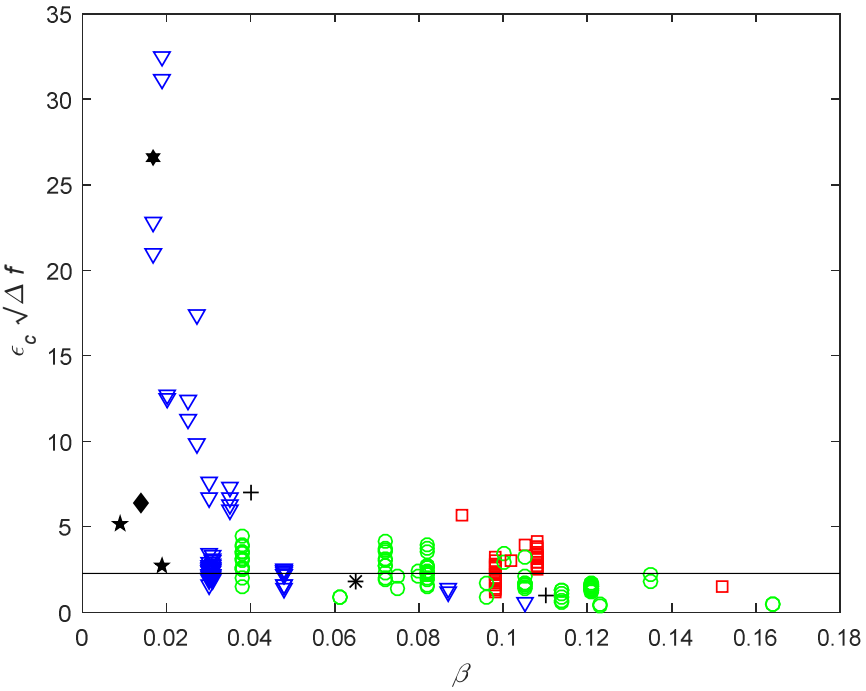

Figure 2: The "universal constant", $\hat{\varepsilon}_c\sqrt{\Delta f}$, from the Huntley et al. (1977) model plotted against beach gradient β. The symbols are identified in Figure 1. The horizontal line shows $\hat{\varepsilon}_c\sqrt{\Delta f}$=2.25 (After Hughes et al., 2014).

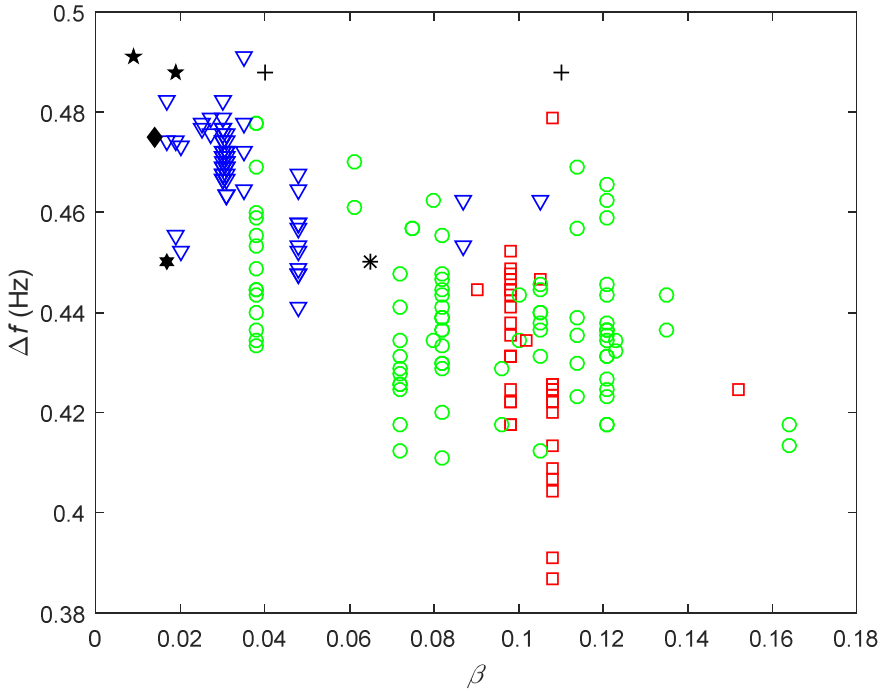

Figure 3: The bandwidth of the f^{-4} roll-off region Δf plotted as a function of the beach gradient β. The symbols are identified in Figure 1.

Figure 4 shows data for an experiment on a bar trough beach in which incident waves measured immediately seaward of the swash zone steadily increased over several hours. The swash variance clearly increased with the surf variance and the swash variance was below the theoretically expected saturation value. Despite no evidence that the surf or swash were saturated in this experiment, the swash spectra displayed an f^{-4} roll-off band.

The swash height and frequency pair for all 13,150 individual swash cycles in the available time series are plotted in Figure 5, together with the theoretical limiting (saturated) swash height predicted by the monochromatic standing wave and bore-driven models for swash. Two versions of the standing wave model are shown. The first is based on a value of unity for the swash scaling parameter ε, which corresponds to the theoretical wave breaking criterion. The other corresponds to a value 3, which the laboratory data of Guza and Bowen (1976) suggests is the critical value at which monochromatic waves saturate.

None of the theoretical/empirical curves in Figure 5 appear to define a limiting swash height for the data analysed here. The standing wave model with a value of ε_c =1 approximates the middle of the data scatter, whereas the curve for ε_c=3 and the curve for the bore-driven model approximate the upper side of the data centroid. Percentages of data that fall above the predicted saturation curves in Figure 5 are listed in Table 1. Approximately 20% of the full data set falls above the saturated swash height predicted by the bore driven model whereas as 72% (12%) falls above the standing wave model prediction for the theoretical value ε_c=1 (empirical value ε_c=3).

Table1. Percentage of data in Figure 5 lying above the predicted limiting (saturated) swash height for the bore-driven and standing wave models for swash.

	Ballistic model	Standing wave model	
		ε_c = 1	ε_c = 3
All data	20	72	12
Reflective	16	61	9
Intermediate	26	75	18
Dissipative	15	76	8

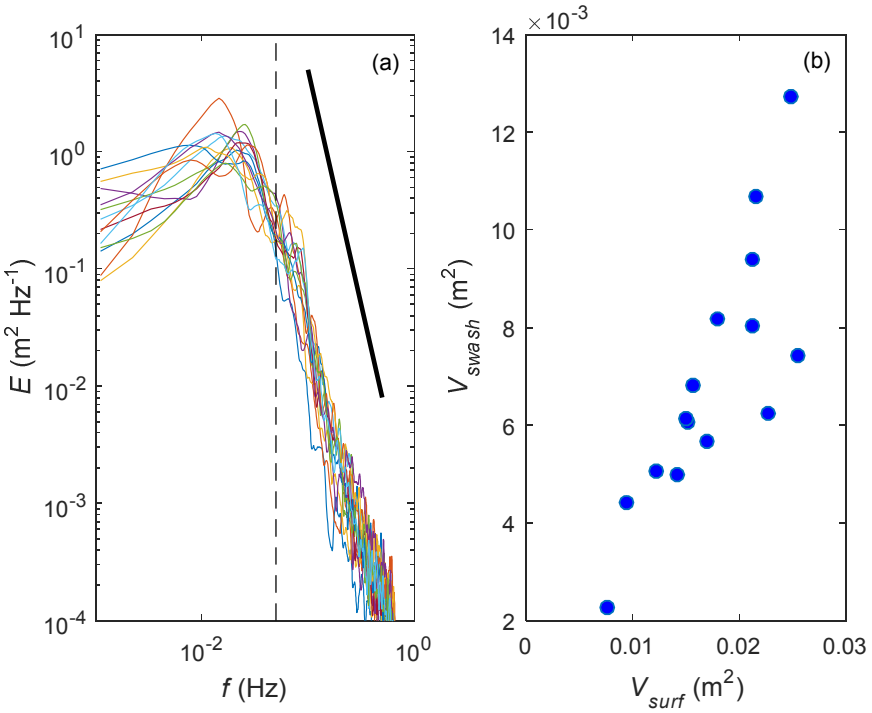

Figure 4: (a) Swash spectra for 15 runs from Stradbroke Island during a rising tide. (b) Scatter plot of the variance in the swash elevation time series (*Vswash*) as a function of that in the inner surf zone (*Vsurf*). Variance in both cases was only calculated over the short wave frequency band (f>0.05 Hz).

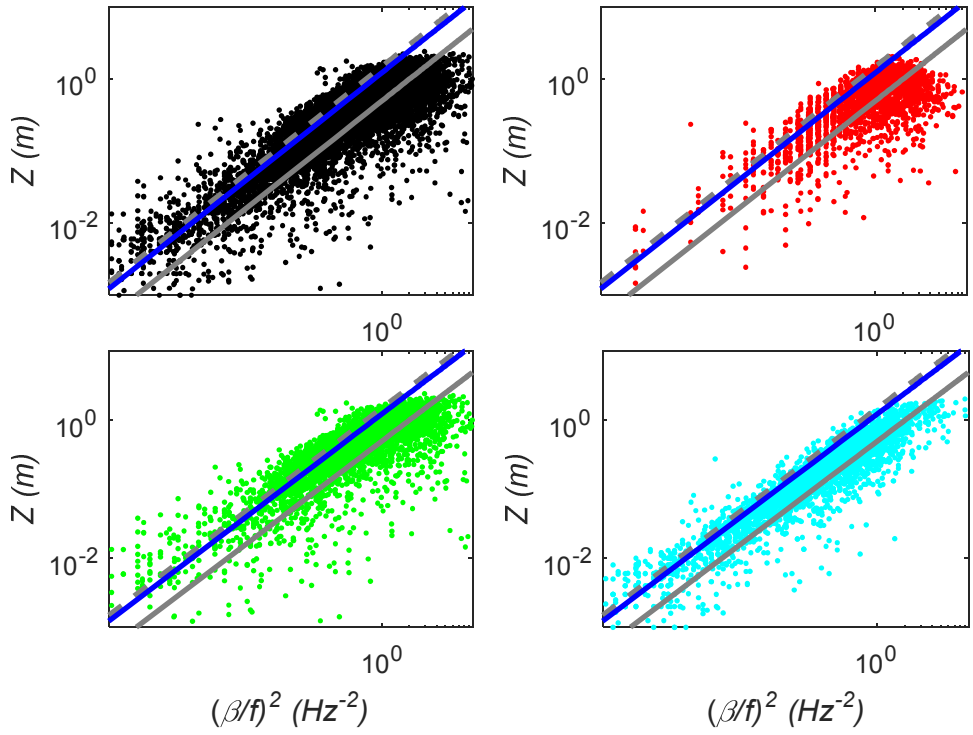

Figure 5: Scatter plots of swash height (Z) against $(\beta/f)^2$ for each individual swash cycle in all the available time series (black); and time series from reflective (red), intermediate (green) and dissipative (cyan) beaches. The limiting swash height according to the bore-driven (blue) and standing wave (grey) swash models is also shown. For the latter the solid line is ε_c =1 and dashed line ε_c =3.

5. Discussion

Several previous studies have measured swash during periods of increasing incident wave energy and found the swash energy in the short-wave frequency band (>0.05 Hz) to be constant (e.g. Guza and Thornton, 1982; Holman, 1983; Aagaard, 1990), which by definition means the short-wave swash was saturated.

The broad-banded version of the standing wave model for saturated swash predicts: (i) an f^{-4} energy roll-off in the saturated part of the spectrum; (ii) the saturated energy level to vary with beach gradient to the fourth power; and (iii) the swash scaling parameter to be a constant. More specifically, the beach gradient, β, and the band width over which wave breaking occurs, Δf, should vary inversely to maintain $\varepsilon_c \equiv \hat{\varepsilon}_c \sqrt{\Delta f} = 1$.

Regarding (i), numerous studies (e.g. Guza and Thornton, 1982; Mizuguchi, 1984; Raubenheimer and Guza, 1996; Ruessink et al., 1998; Holland and Holman, 1999; Ruggiero et al., 2004; Senechal et al., 2011; Guedes et al., 2013), including that by Hughes et al. (2014) which covered the full range of beach types, indicate swash spectra characteristically display an f^{-4} energy roll-off region.

Regarding (ii), the bulk of the data presented here indicates that the swash energy level in the f^{-4} roll-off band varies with beach gradient to the fourth power, although there is a great deal of scatter (Figure 1). See also Raubenheimer and Guza (1996). This scatter might be explained in part by the high power. It might also be explained if the energy in the f^{-4} roll-off band was not saturated in all cases (see below). On low gradient, dissipative beaches the β^4 dependency appears to break down (Figure 1). See also Ruessink et al. (1998).

While Huntley et al. (1977) directly estimated the frequency bandwidth over which wave breaking occurred in their study, it has been a common assumption subsequently that the bandwidth for wave breaking is equivalent to the bandwidth of the f^{-4} energy roll-off. Regarding (iii), the data presented here indicates that β and Δf do vary inversely (Figure 3), thus the inferred frequency bandwidth over which wave breaking occurs increases (in the down-frequency direction) as the beach gradient decreases. Furthermore $\hat{\varepsilon}_c \sqrt{\Delta f}$ was constant for much of the data presented here (Figure 2), but at a value of 2.25±1.72 rather than unity. The value for $\hat{\varepsilon}_c \sqrt{\Delta f}$ is apparently not constant on very gently sloped, dissipative beaches.

While the predicted behavior of the saturated part of the swash spectrum is broadly consistent with the standing wave model for swash saturation, the limiting energy level based on $\varepsilon_c \equiv \hat{\varepsilon}_c \sqrt{\Delta f} = 1$ is underestimated by a factor at least 2 to 3, and more for low gradient dissipative beaches. This is evident by the value $\hat{\varepsilon}_c \sqrt{\Delta f}$ =2.25±1.72 in Figure 2. It is also evident in the wave-by-wave analysis shown in Figure 5, where the amount of data above the predicted limiting swash height is more than 70% for ε=1. Our results are broadly consistent with the data of Guza and Bowen (1976), which showed monochromatic swash saturating at a value of ε=3 rather than 1. Although in our data there is still 12% of the full data set plotting above that saturation line (Table 1).

Our wave-by-wave analysis demonstrates the bore-driven model for saturated swash also underestimated the limiting (saturated) swash height, but by a smaller margin than the standing wave model with the theoretical value ε_c=1 (Figure 5; Table 1). Only 20% of the total data set was above the predicted bore-driven saturation line. Given that the data in Figure 5 was collected across 36 separate field deployments from 9 beaches, it is encouraging that 80% of the data falls below the saturation line.

Measurement accuracy no doubt explains many of the observations plotting above the saturation line of both models, and also the three-dimensionality of natural swash; note the greater occurrence of data falling above the saturation lines on intermediate beaches that have complex beach face topography (Table 1). But there are likely to be factors directly related to the models as well.

The broad-banded version of the standing wave swash model assumes that individual frequencies in the wave breaking band behave independently. This is probably not the case and non-linear interaction between standing waves of different frequencies may partially explain underestimation of the saturated swash energy. Application of the theoretical value ε_c=1 for the onset of breaking is also a probable explanation. There is noticeable hysteresis in the wave breaking process over natural surf zone topographies (Cowell, 1982). Energy dissipation by wave breaking and reflection coefficients are therefore likely to be more complex on natural beaches than suggested by Equation 1, and this is evident in the laboratory data present by Guza and Bowen (1984) where there was a broad transition region ($1<\varepsilon<3$) in

swash response to breaking waves.

On one level, the bore-driven swash saturation model allows for interaction between waves of different frequencies, in that the onset of saturation is defined by the onset of wave-swash interactions. In solving for the limiting swash height, however, the model assumes that each individual wave behaves independently. It does not predict a change in the limiting swash height due to waves interacting, the limiting swash height is predicted to be the maximum possible swash height without wave-swash interactions occurring.

There are two modes of wave-swash interaction of interest here. The first, called wave-uprush interaction, where the second wave overtakes the front of the first wave during the first wave's uprush stage. The second, called wave-backwash interaction, where the second waves overruns the swash lens of the first wave during the first wave's backwash stage (Erikson et al. 2005; Hughes and Moseley, 2007). Wave-backwash interactions will likely reduce the swash height resulting from the second wave, which is the mechanism for saturating the swash in the bore-driven model (Baldock and Holmes, 1999).

In the bore-driven swash model wave-uprush interactions are assumed to have no impact on the swash height, since the overtaking bore is expected to collapse upon reaching the 'dry' beach and the swash height is measured from the collapse point. In reality, the travel of the bore over the preceding uprush may result in the subsequent shoreline motion departing from a ballistic description, particularly if the overtaking bore receives a push from the following water as it arrives at the 'dry' beach.

Erikson et al. (2005) refined the bore-driven swash model to include wave-swash interactions. While the approach was necessarily simplified, it demonstrated that the largest swash heights are often not associated with the largest bore heights. While this type of non-linear behavior can be investigated with numerical models it is not clear whether they will lead to a straightforward expression for a limiting swash height, but the approach shows promise.

Both models predict an f^{-4} energy roll-off region for saturated swash. In the standing wave case, the roll-off band corresponds to the frequency band of breaking waves, and in the bore-driven case it corresponds to the frequencies for which wave-swash interactions are occurring. This raises the question – is an f^{-4} energy roll-off a sufficient condition for inferring swash saturation, and therefore is swash in the short-wave frequency band universally saturated? Figure 4 suggests that it is not a sufficient condition and the degree of scatter in Figure 2 and 5 below the limiting swash energy level (height) suggest that short-wave swash saturation is not universal on natural beaches. In the standing wave case, this is consistent with the surf not being universally saturated (e.g. Baldock et al., 1998; Power et al., 2010).

6. Summary and Conclusion

Swash behaviour has been investigated systematically across the full range of microtidal, sandy beach types from reflective through to dissipative. At the reflective end of the continuum swash energy was predominantly in the frequency band directly associated with incident sea and swell. At the dissipative end of the continuum swash energy was predominantly in the infragravity frequency band.

Two theories for swash saturation were investigated, herein referred to as the standing wave model and the bore-driven model. The former assumes surf saturation which results in swash saturation, whereas the latter assumes swash saturation when bore-swash interactions occur.

Both theories predict that the limiting (saturated) swash height for monochromatic incident waves is directly proportional to the beach gradient squared, inversely proportional to the frequency squared, and independent of incident wave height. Broad-banded versions of the models predict the same proportionalities, but to the fourth power. Based on these model predictions it is generally assumed an f^{-4} energy roll-off at the high frequency end of the spectrum indicates swash saturation across that frequency band.

The data set demonstrated that swash across a wide range of beach types displayed behavior consistent with predictions for swash saturation in the short-wave frequency band, which is generally considered to correspond with wave breaking. For example:

1. A spectral energy roll-off at f^{-4} at the high-frequency end of the spectrum was ubiquitous across all beach types.
2. The total spectral energy in the f^{-4} roll-off band varied with beach gradient to the fourth power.
3. The width of the f^{-4} roll-off band, Δf, varied inversely with beach gradient.

4. The swash scaling parameter $\varepsilon_c \equiv \hat{\varepsilon}_c \sqrt{\Delta f}$ was approximately constant across a wide range of beaches.

Despite the consistency observed between data and model predictions at the broad level, the devil is in the detail, and there are significant issues still to be resolved before we have a robust model for swash saturation.

1. Both available models for swash saturation under-predict the limiting swash energy level or limiting swash height.
2. In addition to swash spectra that are understood to be saturated, an f^{-4} frequency roll-off in the short wave band also occurs in swash spectra that are not saturated.
3. On very flat, dissipative beaches the f^{-4} roll-off region (and inferred saturation) can extend well into the infragravity wave band, which is not consistent with the standing wave model for swash saturation, despite infragravity waves likely to be standing waves.
4. The two available models predict a factor 2.5 difference in the limiting swash height.

These unresolved issues represent a gap in our understanding of beach behavior and limits the ability to predict magnitudes and relative contributions of short and long waves to morphological change at the beach face during storms. It also limits the ability to predict swash energy levels responsible for beach recovery and therefore the rate of recovery. Improved model approaches that correctly predict wave breaking and the reflection coefficient and account for the broad-banded and non-linear aspects of natural swash are required to resolve the outstanding issues listed above.

Acknowledgements

The Australian Research Council and the Danish Natural Sciences Research Council funded many of the experiments reported here. Colleagues who provided valuable assistance with these experiments at various times include Andrew Aouad, Nick Cartwright, Aaron Coutts-Smith, David Hanslow, David Mitchell, Adrienne Moseley, Peter Nielsen, Tony Peric, Hannah Power, and Felicia Weir.

References

Aagaard, T., 1990. Swash Oscillations on Dissipative Beaches - Implications for Beach Erosion, *J. Coastal Res., SI9*, 7 38-752.

Aagaard, T., 1991. Multiple-bar morphodynamics and its relation to low-frequency edge waves, *J. Coastal Res., 7*, 801 -813.

Baldock, T.E., and P. Holmes, 1999. Simulation and prediction of swash oscillations on a steep beach, *Coastal Eng., 36*, 219-242.

Baldock, T.E., P. Holmes, S. Bunker, P. van Weert, 1998. Cross-shore hydrodynamics within an unsaturated surf zone, *Coastal Eng. 34*, 173-196.

Battjes, J.A., H.J. Bakkenes, T.T Janssen, and A.R. van Dongeren, 2004. Shoaling of sub-harmonic gravity waves, *J. G eophys. Res., 109*, C02009, doi: 10.1029/2003JC001863.

Carrier, G.F., and H.P. Greenspan, 1958. Water waves of finite amplitude on a sloping beach, *J. Fluid Mech., 4*, 97-109.

Cowell, P.J., 1982. *Breaker Stages and Surf Structure on Natural Beaches*. Coastal Studies Unit Technical Report 82/7, Sydney, Australia.

Erikson, L., M. Larson, and H. Hanson, 2005. Prediction of swash motion and run-up including the effects of swash int eraction, *Coastal Eng., 52*, 285-302.

Guedes, R.M.C., Bryan, K.R., and Coco, G., 2013. Observations of wave energy fluxes and swash motions on a low-slo ping, dissipative beach. J. Geophys. Res., 118, 3651-3669.

Guza, R.T., and Bowen, A.J., 1976. Resonant interactions for waves breaking on a beach. *Proceedings 15th Internation al Coastal Engineering Conference*, ASCE, New York, 560-579.

Guza, R.T., and E.B. Thornton, 1982. Swash oscillations on a natural beach, *J. Geophys. Res., 87*, 483-491.

Holland, K.T., and R.A. Holman, 1999. Wavenumber-frequency structure of infragravity swash motions, *J. Geophys. R es., 104*, 13,479-13488.

Holland, K.T., and J.A. Puleo, 2001. Variable swash motions associated with foreshore profile change, *J. Geophys. Res., 106*, 4613-4623.

Holland, K.T., B. Raubenheimer, R.T. Guza, and R.A. Holman, 1995. Run-up kinematics on a natural beach, *J. Geophy s. Res., 100*, 4985-4993.

Holman, R.A., 1983. Edge waves and the configuration of the shoreline, in *CRC Handbook of Coastal Processes and E rosion*, edited by P.D. Komar, pp. 21-33, CRC Press Inc., Boca Raton, Florida.

Hughes, M.G., 1992. Application of a non-linear shallow water theory to swash following bore collapse on a sandy bea ch, *J. Coastal Res*., *8*, 562-578.

Hughes, M.G., and A.S. Moseley, 2007. Hydrokinematic regions within the swash zone, *Cont. Shelf Res.*, 27(15), 2000-2013.

Hughes, M.G., Aagaard, T., Baldock, T.E., and Power, H.E., 2014. Spectral signatures for swash on reflective, intermed iate and dissipative beaches. *Marine Geology*, 355, 88-97.

Huntley, D.A., 1976. Long-period waves on a natural beach, *J. Geophys. Res.*, *81*, 6441-6450.

Huntley, D.A., R.T. Guza, and A.J. Bowen, 1977. A universal form for shoreline run-up spectra?, *J. Geophys. Res*., *82*, 2577-2581.

Kemp, P.H., 1975. Wave asymmetry in the nearshore zone and breaker area, in *Nearshore Sediment Dynamics and Sedi mentation*, edited by J. Hails and A, Carr, pp. 47-65, Wiley.

Mase, H., 1988. Spectral characteristics of random wave run-up, *Coastal Eng*., *12*, 175-189.

Miche, R., 1944. Mouvement ondulatoires de mers en profondeur constante ou decroissante, *Ann. Ponts Chaussees*, *11 4*, 25-78.

Miche, R., 1951. Le pouvoir reflechissant des ouvrages maritimes exposes a l'action de la houle, *An. Ponts Chaussees*, *121*, 285-319.

Mizuguchi, M., 1984. Swash on a Natural Beach, *19th Coastal Engineering Conference*, Am. Soc. of Civ. Eng., Housto n, Texas.

Power, H.E., Hughes, M.G., Aagaard, T., and Baldock, T.E., 2010. Nearshore wave height variation in unsaturated surf. Journal of Geophysical Research, 115, doi:10.1029/2009JC005758.

Raubenheimer, B., and R.T. Guza, 1996. Observations and predictions of run-up, *J. Geophys. Res*., *101*, 25,575-25,587.

Ruessink, B.K., M.G. Kleinhans, and P.G.L. van den Beukel, 1998. Observations of swash under highly dissipative con ditions, *J. Geophys. Res*., *103*, 3111-3118.

Ruggiero, P., R.A. Holman, and R.A. Beach, 2004. Wave run-up on a high-energy dissipative beach, *J. Geophys. Res*., *109*, C06025, doi:10.1029/2003JC002160.

Senechal, N., Coco, G., Bryan, K.R., and Holman, R.A., 2011. Wave runup during extreme storm conditions. J. Geophy s. Res., 116, C07032, doi:10.1029/2010JC006819.

Shen, M.C., and R.E. Meyer, 1963. Climb of a bore on a beach - Part 3. Run-up, *J. Fluid Mech*., *16*, 113-125.

Waddell, E., 1976. Swash-groundwater-beach profile interactions, in *Beach and Nearshore Sedimentation*, edited by R. A. Davis Jr. and R.L. Ethington, pp. 115-125, Society of Economic Paleontologists and Mineralogists.

Wright, L.D., and A.D. Short, 1984. Morphodynamic variability of surf zones and beaches; a synthesis, *Mar. Geol*., *56*, 93-118.

Yeh, H.H., A. Ghazali, and I. Marton, 1989. Experimental study of bore run-up, *J. Fluid Mech*., *206*, 563-578.